GRC Transactions, Vol. 42, 2018

# Which Geologic Factors Control Permeability Development in Geothermal Systems? The Geologic Structure of Dixie Valley

**Drew L. Siler and Jonathan M.G. Glen**

**U.S. Geological Survey, Menlo Park, CA, USA**

**Keywords**

*Structure, Dixie Valley, faults, upwelling, gravity, magnetic, geothermal, potential field, permeability, fault, fracture*

## ABSTRACT

Geothermal systems occur where subsurface permeability and temperature are sufficiently high to drive fluid circulation. In the Great Basin region of the United States, which hosts ~20% of domestic geothermal electricity generation capacity and much of the projected undeveloped and undiscovered resource, crustal heat flow is relatively high, so permeability is the dominant factor controlling the occurrence or absence of a geothermal system. In the most general sense, fracture permeability along faults and/or networks of interconnected faults and fractures serves as a pathway for fluids upwelling from depth. Within the Great Basin, Dixie Valley hosts an anomalously high number of geothermal systems. It is unclear whether this relatively dense collection of systems is associated with regional strain or structural patterns, local structural or geological characteristics, basin hydrogeology, or some other factors. The relatively rich data-set available for Dixie Valley, and the well-studied nature of the area affords the opportunity to characterize the geologic and lithologic factors that control permeability development at the local scale. There are at least eleven distinct geothermal systems in Dixie Valley, NV. We utilize a wealth of existing data, which have been collected over several decades, to assess the geologic controls on geothermal fluid upwelling in these systems.

## 1. Introduction

Dixie Valley is an ~100 km-long, ~15 km-wide north-northeast trending basin in west central Nevada (Figure 1). The valley lies within a relatively broad, northeast trending zone characterized by relatively high heat flow, internally consistent structural trends dominated by northeast striking fault systems, and broad gravity anomalies that is referred to as Humboldt structural zone (Rowan and Wetlaufer, 1981). This area is also associated with relatively high strain rates (Kreemer et al., 2009, 2012; Hammond et al., 2014), the Central Nevada Seismic Belt, a ~north-northeast striking area of anomalously high rates of Historic-Holocene seismicity, relative to the surrounding basins (Bell et al., 2004), relatively high $^{3}He/^{4}He$ ratios in geothermal waters (Kennedy and van Soest, 2006, 2007; Siler and Kennedy, 2016), and a relatively high density of geothermal systems (Faulds et al., 2004).

Historic tectonic activity in Dixie Valley is demonstrated by scarps from the 1954 Dixie Valley earthquake that extend for ~50 km in the southern part of the valley ($M_s$ 6.8; Slemmons, 1957; Caskey et al., 1996). Additionally, scarps from the 1915 Pleasant Valley earthquake ($M_s$ 7.6; Wallace, 1984) extend through the Sou Hills area at the northern end of Dixie Valley, and scarps from the 1954 Fairview Peak ($M_s$ 7.2; Slemmons, 1957; Caskey et al., 1996) extend into Dixie Valley as far as the Pirouette Mountain area from the south. Research associated with these earthquakes, geothermal exploration and development, oil and gas exploration, and research associated with regional tectonics and volcanism has resulted in a wealth of publicly available surface and subsurface data in Dixie Valley.

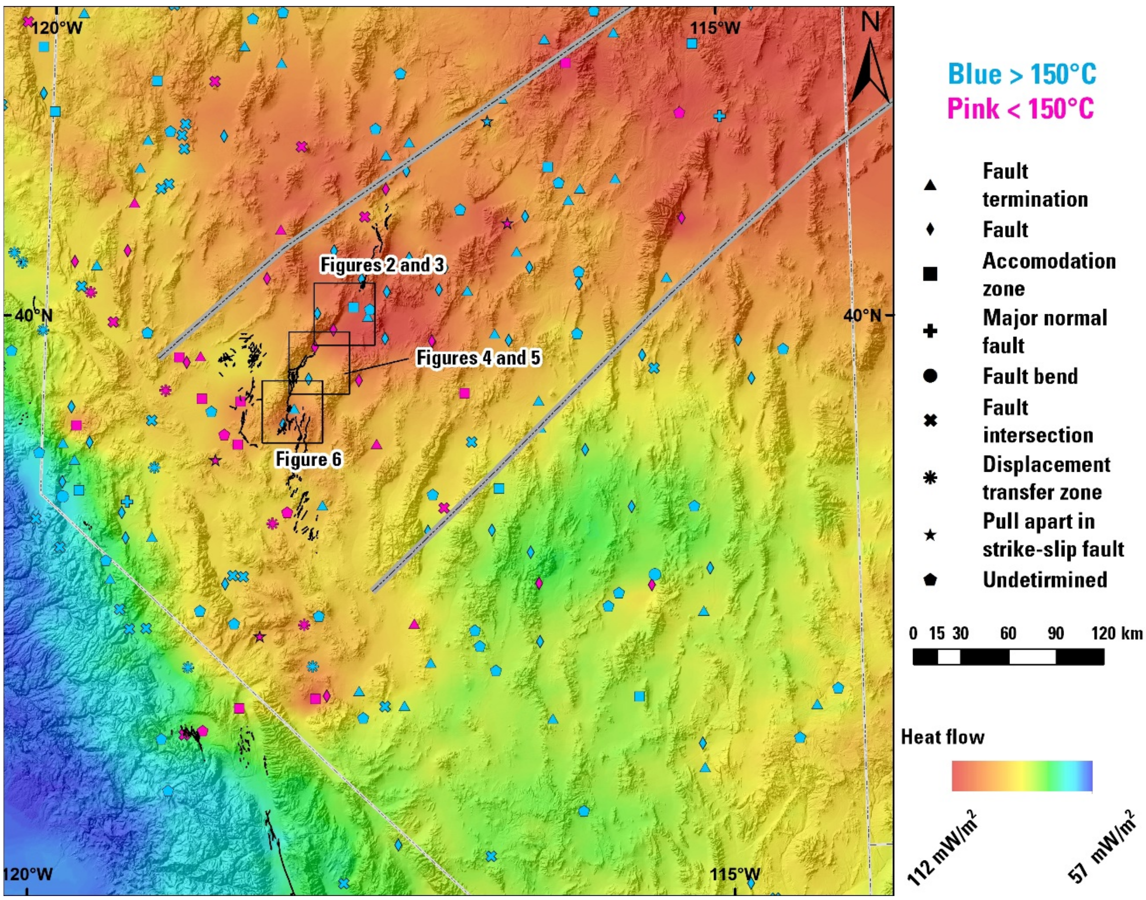


**Figure 1: Regional map of central Nevada. Heat flow from Williams and DeAngelo (2011), geothermal system structural settings from (Faulds et al., 2011; Faulds and Hinz, 2015). Historic faults are shown, representing the Central Nevada Seismic belt. Grey lines indicate the boundaries of the Humboldt structural zone as defined by Rowan and Wetlaufer (1981)**

At least eleven geothermal systems are known to occur in Dixie Valley (Benoit, 2011; Bergman et al., 2015). These have been identified based on surface geothermal occurrence and shallow and deep temperature data. These eleven systems appear to be geochemically and hydrogeologically distinct from one another (Bergman et al., 2015). This paper builds upon several decades of research in Dixie Valley and several recent compilations and syntheses Dixie Valley data (Benoit, 2011; Iovenitti et al., 2013; Bergman et al., 2015). We re-examine the geological setting of eleven Dixie Valley geothermal systems as characterized by existing and publicly available geological and geophysical in the valley to document basin structure, assess whether there are structural and/or geologic factors that are common to the different geothermal systems, and to gain and understanding of why the valley hosts a seemingly high concentration of systems.

Gravity data used in this study are a compilation of a number of different datasets, predominantly from the Gravity Map of Nevada (Ponce, 1997), and publicly available data compiled by Iovenitti et al., (2013). Station spacing is variable, but in most of the areas of geothermal interest spacing is on the order of ~1 km or finer. Data were reduced to the Bouger anomaly using a reduction density of 2.67 g/cc and applying standard methods (Blakely, 1996). Magnetic data used in this study are from a ~940 km$^2$ high-resolution helicopter aeromagnetic survey with west-northwest-to-east-northeast oriented flight lines, line spacing of 200 m (orthogonal tie lines space at ~1000 m) and an observation height of 120 m above the ground (Grauch, 2002). Thirty-one 2D seismic reflection lines in northern Dixie Valley were consulted in the study. Reflection profiles from (Bergman et al., 2015) were re-interpreted as part of this study. Existing 2D reflection interpretations presented in (Faulds et al., 2016, 2017) were also utilized. Several geologic maps at a variety of scales (Muller et al., 1951; Page, 1965; Speed, 1976; John, 1995a, 1997; Plank, 1997) were compiled and integrated with new mapping in order to constrain the bedrock geology in the ranges

## 2. Geothermal systems in Dixie Valley

There are at least eleven known geothermal systems in Dixie Valley (Faulds et al., 2006, 2011; Benoit, 2011; Bergman et al., 2015). Although some are referred to by several names in the literature, we refer to them here with what we consider their most common names. The geothermal systems are: McCoy hot springs, Sou Hills (aka Seven Devils), Western Augustana Mountains Ranch hot springs (aka Lower Ranch), Hyder hot springs, Dixie Valley geothermal field, Coyote Canyon (aka Dixie Valley Power Partners), Dixie Comstock, Dixie Meadows (aka Dixie hot springs), Clan Alpine Ranch, Pirouette Mountain, and Eleven Mile Canyon.

### *2.1 Sou Hills*

The Sou Hills geothermal area is located at the northern end of Dixie Valley. Sou hot springs, a collection of thermal springs surrounded by travertine deposits is located ~6 km east of the Stillwater Range front (Figure 2). The springs have a discernable north-northeast trend. Fluids as hot as 76°C have been measured at the surface (Benoit, 2011), with multi-component geothermometry as high as 160°C (Faulds et al., 2016, 2017). Sou Hills is one of the focus areas of the Nevada play-fairway analysis project (Faulds et al., 2016). As part of the play-fairway analysis project new geologic mapping, collection and interpretation of LiDAR data, collection of 355+ new gravity stations, collection of a 2 m temperature data, and interpretation of existing seismic reflection profiles were conducted (Faulds et al., 2017).

The Sou Hills area occupies a ~10-km wide accommodation zone between the east-dipping Dixie Valley fault system (as young as 2.2-2.5 ka at (Caskey et al., 2004) or certainly younger than late-Pleistocene <15,000 yrs (U.S. Geological Survey, 2006) at the latitude of Sou Hills) to the south and the west-dipping Pleasant Valley fault system (late-Pleistocene <15,000 yrs at the latitude of Sou Hills, with 1915 ruptures ~10 north (U.S. Geological Survey, 2006)) to the north.

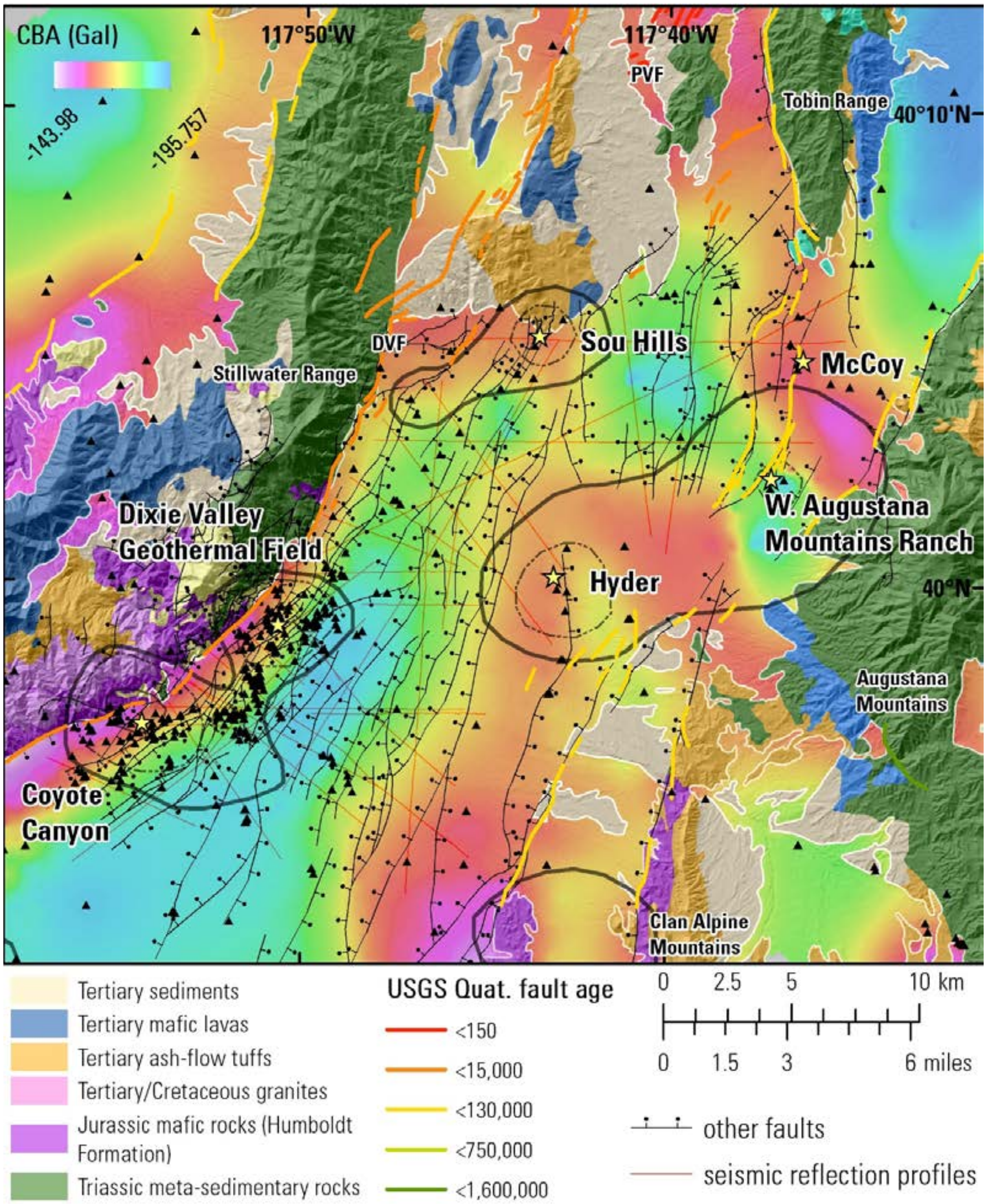


**Figure 2. Gravity and geologic map of northern Dixie Valley. Bouger gravity anomaly is shown, warm colors indicate gravity highs, cool colors gravity lows. Faults (U.S. Geological Survey, 2006) and structural interpretations of geophysical and geologic data associated with this study are shown. Geology in the ranges from a compilation of maps including (Muller et al., 1951; Page, 1965; Speed, 1976; John, 1995a, 1997; Plank, 1997) and mapping associated with this study. Black triangles indicate geothermal and temperature gradient wells. Temperature gradient contours shown are from (Bergman et al., 2015), thick black line is the 80°C/km contour, dashed line is the 120°C/km contour.**

**Table 1. General characteristics of the eleven geothermal systems in Dixie Valley. See text for citation information**

| | Deposits and or surface features | Max measured temperature | Max geothermometry | Host lithology | Maximum Explored depth | Fault systems | Fault system age | fault system strike | dip direction; dip azimuth | Structural setting | Magnetic anomoly |
|---|---|---|---|---|---|---|---|---|---|---|---|
| **Sou Hills** | springs; travertine | 76°C (surface) | 160°C (multicomponent) | Triassic metaseds, Tertiary ash-flow tuffs and basalts | ~450 m | Pleasant Valley fault and Dixie Valley fault | Holocene-Historic | ~005 | west; normal | Accomodation zone | -- |
| **McCoy hot spring** | springs | 46°C (surface) | 57°C (Na-K-Ca and chalcedony) | Triassic metaseds, Tertiary ash-flow tuffs | ~150 m | Pleasant Valley fault(?) Tobin Range fault; Augustana Mts fault | <mid-Pleistocene | ~010 | west; normal(?) | Fault termination | -- |
| **Western Augustana Mountains** | springs; travertine on top of silica | 40°C (surface) | ~62°C (Na-K-Ca and chalcedony) | Triassic metaseds | surface | Pleasant Valley fault(?) Tobin Range fault; Augustana Mts fault | <mid-Pleistocene | ~010-025 | west; normal (?) | Fault termination; fault step-over; fault intersection | -- |
| **Hyder hot spring** | springs; travertine | 62°C (surface); 71°C (@350 m) | ~77-88°C (Na-K-Ca and chalcedony) | Humbodlt Formation? | 500 m | Clan Alpine Mts fault; Augustana Mts fault | <mid-Pleistocene | ~025 | east and west; normal (?) | Fault termination; fault step-over | Local mag low (?) |
| **Dixie Valley geothermal field** | fumaroles | ~250°C (reservoir temperature) | -- | Humboldt Formation, Triassic metaseds | ~3800 m | Dixie Valley 'piedmont fault' | <late-Pleistocene | ~045 | east and west; normal | Accomodation zone | Local mag low |
| **Coyote Canyon** | fumaroles, travertine cemented seds | 285°C (@ 3000 m) | -- | Humboldt Formation, Triassic metaseds | ~3500 m | Dixie Valley 'piedmont fault' | <late-Pleistocene | ~045-070 | east; normal | Fault step-over | Local mag low |
| **Dixie Comstock** | silica sinter | 196 °C (@ 2750 m) | 196 °C (method?) | Triassic shales | ~2700 m | Dixie Valley 'piedmont fault' | <late-Pleistocene | ~350-000 | east; normal | Fault step-over | Local mag low |
| **Dixie Meadows** | springs, fumeroles | 83°C (surface); 144 (@ 70 m) | 116-143°C (quartz and Na/K/Ca) | Triassic meta-seds, Tertiary ashflow-tuffs | 500 m (?) | Dixie Valley 'piedmont fault' | Historic | ~045 | east; normal | Fault step-over | Local mag low |
| **Clan Alpine Ranch** | -- | 72°C (@70 m) | -- | Triassic meta-seds, Tertiaty granites, Tertiary ashflow-tuffs | 70 m | Clan Alpine Mts fault | <mid-Pleistocene | ~000-040 | west;normal | Fault step-over | -- |
| **Pirouette Mountain** | -- | 87°C (@600 m); 85°C (@ 2250 m) | -- | Tertiary ash-flow tuffs and Tertiary granites | 2250 m | Gold King fault, Louderback Mts. fault, Dixie Valley fault, West Gate fault | Historic | ~000-015 | east and west; dextral normal, normal | Accomodation zone | -- |
| **Eleven Mile Cayon** | -- | 80°C (@600 m) | -- | Triassic meta-seds, Tertiaty granites, Tertiary ashflow-tuffs | 2500 m | Gold King fault, Louderback Mts fault, Dixie Valley fault, West Gate fault | Historic | ~000-015 | east and west; dextral-normal, normal | Accomodation zone | -- |

The anticlinal accommodation zone is expressed as two gravity lows with a central, broad gravity high (Figure 2) and by multiple east- and west-dipping normal faults (Faulds et al., 2017). The surficial expression and temperature anomaly lies near the central hinge of the anticline and appears to be associated with several west-dipping faults, which are antithetic to the dominant east-dipping faults on the western side of the anticline (Faulds et al., 2017). Exposures to the north suggest that the fault system is hosted in Tertiary rhyolitic and basaltic volcanic rocks, though the thickness of the Tertiary volcanic is not well constrained. Triassic meta-sedimentary rocks exposed to the north, east, and west in the Tobin Range, Augustana Mountains, and Stillwater Range probably are present in the crystalline basement at deeper levels.

### *2.2 McCoy hot springs and Western Augustana Mountains Ranch hot springs*

McCoy hot springs is located at the north end of Dixie Valley on the eastern side. Geothermal fluid at ~46°C (Goff et al., 2002) discharges into a pool ~30 m in diameter. There are no known travertine or sinter deposits at McCoy (Benoit, 2011) and Bergman et al., (2015) do not show a temperature anomaly associated with McCoy hot springs, though there are ~150 m-deep temperature gradient wells with maximum temperature reported as 46°C in within 1 km of the hot springs (publicly available data, Nevada Division of Minerals).

Western Augustana Mountains Ranch hot springs is located ~5 km south-southeast of McCoy hot springs. ~40°C geothermal fluids effuse from a ~ 2 km long travertine terrace. A small amount of siliceous sinter is located at the base of the terrace (Goff et al., 2002). Measured and geothermometry temperatures in both systems are relatively low, suggesting that both may be relatively shallow groundwater systems, rather than deeply rooted systems (Goff et al., 2002). The travertine terrace at Western Augustana Mountains Ranch is clearly fault controlled, so despite the likelihood that neither system is associated with deeply rooted upwelling, structure apparently remains a controlling factor in the localization of relatively cooler, shallow geothermal systems.

Both McCoy and Western Augustana Ranch hot springs lie along a younger than mid-Pleistocene (<130,000 yrs) fault system (U.S. Geological Survey, 2006) that bounds the western side of the Tobin Range. Both geothermal systems may also be associated with the fault system along the western side of the Augustana Mountains (mid-Pleistocene (<130,000 yrs)) which bounds the eastern side of Dixie Valley and may link to the mid-Pleistocene Jersey Valley fault to the north. The western Tobin Range fault system may terminate near Western Augustana Mountains Ranch hot springs. Alternatively, he western Tobin Range fault system may the Augustana Mountains fault system may intersect ~5 km south of Western Augustana Mountains Ranch hot springs (Figure 2). Additionally, Western Augustana Ranch hot springs occurs at the north end of a ~10 km-wide right step in the Augustana Mountains fault system, though this wide of a step-over may be too wide to generate the dense, interconnected faults and fractures that are conducive to hosting geothermal fluid flow (e.g., Siler et al., 2018). Outcrop extent suggests that the crystalline basement beneath McCoy and Western Augustana Mountains Ranch consists of Triassic meta-sedimentary rocks, with possible overlying Tertiary volcanic rocks. Outcrop extent of the Jurassic Humboldt Formation suggest that they do not lie beneath the either system (Figure 3).

### *2.4 Hyder*

The Hyder geothermal system is located ~10 km east-southeast of Western Augustana Mountains Ranch, and roughly ~10 km from both the Augustana Mountains and Stillwater Range fronts, i.e., the center of the valley. Hyder discharges 62°C geothermal fluids from a large travertine mound. Nearby temperature gradient wells show 71°C isothermal temperatures below ~350 m (Goff et al., 2002; Benoit, 2011; Bergman et al., 2015).

Hyder sits at the northern termination of an east-dipping fault that bounds the western side of prominent gravity and magnetic highs in the middle of Dixie Valley (Figures 2 and 3). Additionally, Hyder lies near the southern end of a ~10 km-wide right step between the west-dipping Clan Alpine Mountains and the Augustana Mountains faults. As noted above this step-over may be too wide to generate the dense network of interconnected faults and fractures required to host geothermal fluid flow (e.g., Siler et al., 2018). Surface scarps along both fault systems suggest that they are younger than mid-Pleistocene (<130,000 yrs) (U.S. Geological Survey, 2006). The highs in both gravity and magnetic data (Grauch, 2002), south of Hyder suggest that the intrabasin high is a significant structural feature. Outcrops in the Stillwater Range and Augusta Mountains, albeit ~10 km away, suggest that Triassic meta-sediments and the Jurassic Humboldt Formation are present at depth beneath Hyder. The magnetic high is also suggestive of the presence of the highly magnetic Humboldt Formation rocks at depth beneath Hyder. Hyder is also located just west of a local magnetic low.

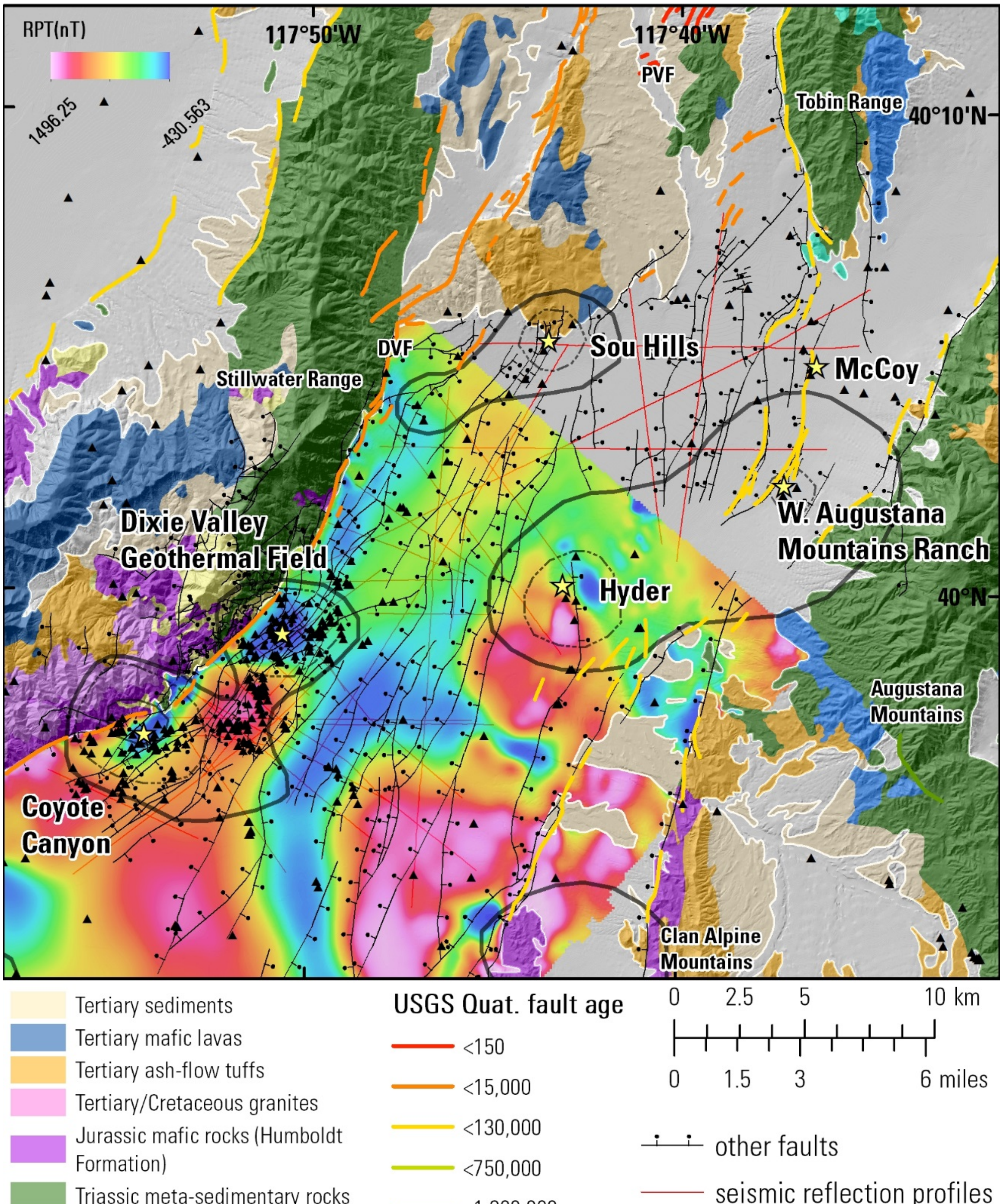


**Figure 3. Magnetic and geologic map of northern Dixie Valley. Reduced to pole magnetic anomaly is shown (Grauch, 2002), warm colors indicate magnetic highs, cool colors magnetic lows. Faults (U.S. Geological Survey, 2006) and interpretations of the geophysical and geologic data associated with this study are shown. Geology in the ranges are compiled from a variety of maps including (Muller et al., 1951; Page, 1965; Speed, 1976; John, 1995a, 1997; Plank, 1997) and mapping associated with this study. Black triangles indicate geothermal and temperature gradient wells. Temperature gradient contours shown are from Bergman et al., (2015), thick black line is the 80°C/km contour, dashed line is the 120°C/km contour.**

### *2.5 Dixie Valley geothermal field*

The Dixie Valley geothermal field extends for at least 6 km along the Stillwater range front. This section of the Dixie Valley fault system has been referred to as the Stillwater seismic gap, as it lies between the 1915 Pleasant Valley ruptures to the north and the 1954 Dixie Valley rupture to the south (Figures 2 and 3). This section of the Dixie Valley fault may have ruptured as recently as 2.2-2.5 ka (Caskey et al., 2004), but is certainly younger than late Pleistocene (<15,000 yrs) (U.S. Geological Survey, 2006). In general, the geothermal well field is ~2 km from the topographic range front. The Senator Fumeroles effuse from the Dixie Valley fault system at the range front near the north end of the geothermal field. Some studies have suggested that geothermal wells produce from the moderately- to shallowly-dipping Dixie Valley range front fault system (Johnson and Hulen, 2002). Gravity, magnetic, and seismic reflection data indicate that production more probably occurs from a relatively steep, ‘piedmont’ fault system that is ~1 km from the topographic range front and not exposed at the surface (Blackwell et al., 2007; Bergman et al., 2015). Production fractures within the piedmont fault system occur predominantly in the mafic igneous rock of the Humboldt Formation which is exposed in the Stillwater Range northwest of the geothermal field (Bergman et al., 2015). In and directly adjacent to the Dixie Valley geothermal field the Triassic meta-sedimentary rocks have invariably low permeability (Bergman et al., 2015) and deep wells penetrating the Triassic section generally display conductive temperature profiles, helping to define the margins of the field (Williams et al., 1997). Magnetic data suggest that the highly magnetic Humboldt Formation lies beneath the geothermal field, and extends across Dixie Valley to where it is exposed in the Clan Alpine Mountains to the southeast of the geothermal field (Figure 3).

The Dixie Valley fault and the piedmont fault system strike along azimuth 045 for ~6 km adjacent to the geothermal field but strike more easterly to the south and more northly to the north of the geothermal field. Furthermore, the geothermal field sits within a ~6 km long, narrow (~4 km wide) graben defined by the east-dipping piedmont fault system to the west and east-dipping faults interpreted from gravity, magnetic, and seismic reflection data to the east (Blackwell et al., 2000; Figure 2). To the north of geothermal field, the west-dipping faults defining the eastern side of the graben appear to terminate into the east-dipping faults of the Sou Hills accommodation zone. To the south of the geothermal field the graben widens significantly, as the west-dipping faults defining the eastern side strike more southerly. The narrowness of the graben at the latitude of the geothermal field is likely an important control on permeability development. The intersection between west-dipping and east-dipping faults bounding and within the graben (Johnson and Hulen, 2002) likely localize permeability associated with deeply derived upwelling (Wisian and Blackwell, 2004; Bergman et al., 2015) and with geothermal production. The northern part of the Dixie Valley geothermal field is associated with a local magnetic low.

### *2.6 Coyote Canyon*

The Coyote Canyon geothermal area lies ~6 km southwest of the Dixie Valley geothermal field. The Section 10/15 fumaroles are located within the Coyote Canyon thermal anomaly and effuse from the Dixie Valley range front fault system. Coyote Canyon contains several deep wells including the hottest bottom hole temperature measured in Nevada, at 285°C (Blackwell et al., 2000). Despite its relative proximity to the Dixie Valley geothermal field, pressure, temperature, and fluid chemistry data suggest that it is disconnect from the producing geothermal system.

The Dixie Valley fault zone at the range front and the piedmont fault system are both evident from potential field data (Figure 2) and surface exposure in the Coyote Canyon area, similar to the Dixie Valley geothermal field to the north. The Dixie Valley fault zone though Coyote Canyon is younger than late-Pleistocene (<15,000 yrs) or perhaps as young at 2.2-2.5 ka (Caskey and Ramelli, 2004; U.S. Geological Survey, 2006). The Dixie Valley fault zone strikes along azimuth 070 through the Coyote Canyon area, whereas gravity and seismic reflection data suggest that the piedmont fault system strikes ~045, roughly equivalent to its strike in the Dixie Valley geothermal field to the north. This change in strike of the Dixie Valley fault occurs as the fault subtly bends ~2 km to the right through the Coyote Canyon area. In the strike-direction the step occurs over a relatively broad area, ~6 km-wide. Gravity data show that the narrow graben hosting the Dixie Valley geothermal field is significantly wider at the latitude of Coyote Canyon, perhaps as wide as 9 km. Even so, west-dipping faults antithetic to and intersecting with the piedmont fault system at depth are evident on seismic reflection data, a similar geometry to the Dixie Valley geothermal field to the north. Geologic mapping, magnetic data, and deep drilling data indicate that the Humboldt Formation, Triassic meta-sedimentary rocks, and possibly Mesozoic granitic rocks occur at depth beneath Coyote Canyon. Magnetic data show a local magnetic low at Coyote Canyon.

### *2.7 Dixie Comstock*

Dixie Comstock is located along the Dixie Valley fault ~12 km southwest of Coyote Canyon. Intense heat at ~30 m depth and near boiling fluids in the Dixie Comstock Mine resulted in an end to gold mining operations there in the 1930s. Eroded siliceous sinter deposits, silicified sediments, and root casts are located adjacent to the mine (Vikre, 1994). Geothermal fluids at 196°C where measured in a deep exploration well located ~1 km east of the mine opening.

The Dixie Valley fault zone strikes along azimuth 350-to-000 along a ~4 km-long segment through the Dixie Comstock area. Most recent slip on the Dixie Valley fault system through Dixie Comstock is younger than late-Pleistocene (<15,000 yrs) (U.S. Geological Survey, 2006), though scarps associated with 1954 Dixie Valley earthquake end just ~5 km to the south of the Dixie Comstock area. Dixie Comstock, therefore is approximately the southern extent of the Stillwater seismic gap. Vikre (1994) documents two piedmont faults ~1 km east of the range front. These faults are evident in gravity and magnetic data (Figure 4 and 5). Dixie Comstock also lies at the southern end of a ~2.5 km wide left-step in the Dixie Valley range front and piedmont fault systems. A local magnetic low occurs at and to the south of Dixie Comstock. The Dixie Valley fault at the Dixie Comstock mine juxtaposes mafic intrusive and volcanic rocks of the Humboldt Formation against Quaternary colluvium, whereas drilling penetrated predominantly Triassic shale (Vikre, 1994). Magnetic data (Figure 5) and geologic mapping suggest that Dixie Comstock lies at the southern extent of the Humboldt Formation in Dixie Valley (e.g., Speed, 1976; Grauch, 2002).

### *2.9 Dixie Meadows*

Dixie Meadows lies along the Stillwater Range front ~9 km south-southeast of Dixie Comstock. Dixie Meadows hot springs discharge from at least 35 springs and seeps in unconsolidated sediments in the area (Bohm et al., 1980). Spring temperatures range from ambient to 83°C. Two fumaroles discharge in the area, one from the alluvial fan ~0.5 km west of the springs and one along the Dixie Valley fault system at the range front (Kennedy-Bowdoin et al., 2004). 144°C was measured at 70 m depth in a temperature gradient well near the springs (Bergman et al., 2015).

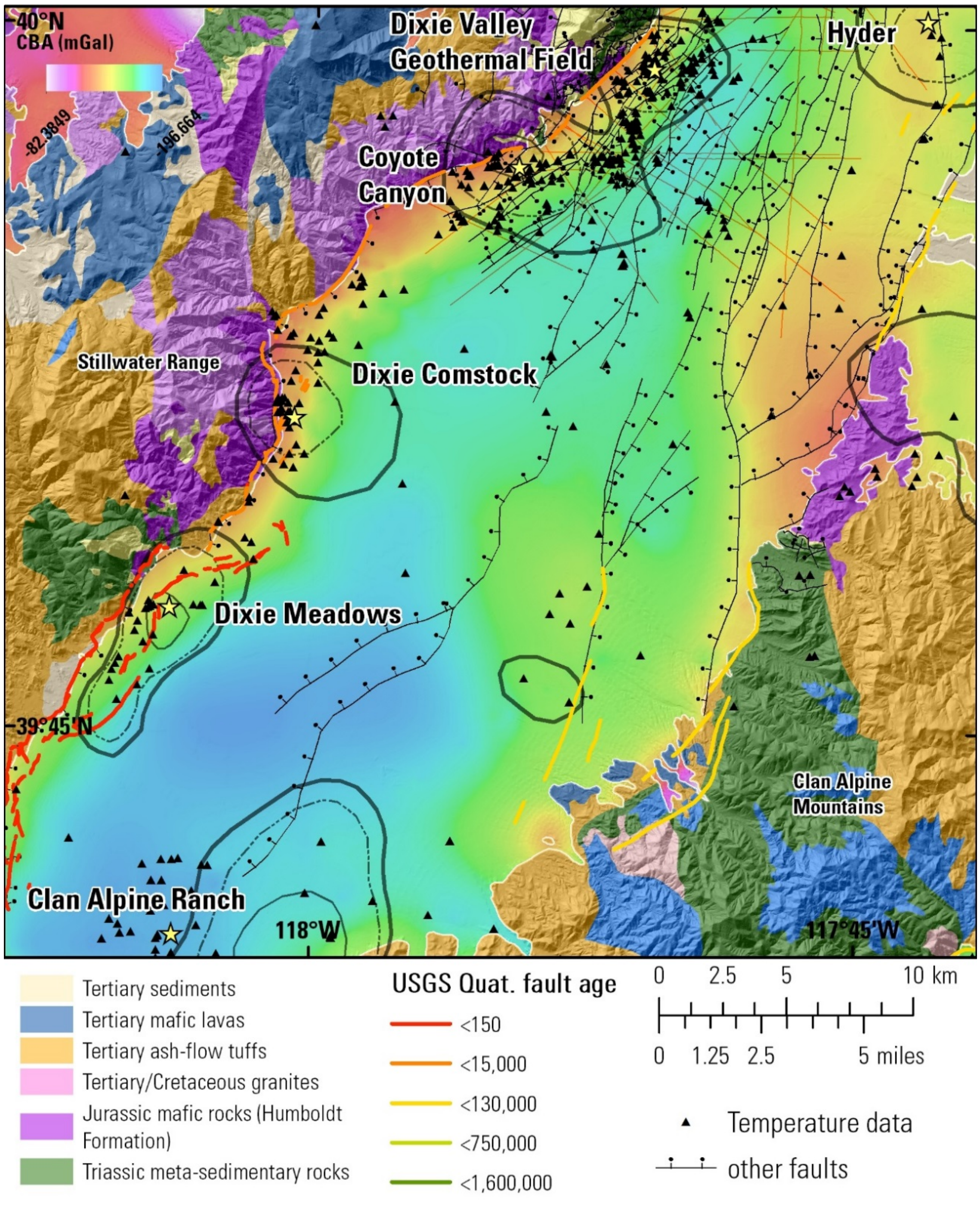


**Figure 4. Gravity and geologic map of central Dixie Valley. Bouger gravity anomaly is shown, warm colors indicate gravity highs, cool colors gravity lows. Faults (U.S. Geological Survey, 2006) and interpretations of geophysical and geologic data from this study are shown. Geology in the ranges from a compilation of maps including (Muller et al., 1951; Page, 1965; Speed, 1976; John, 1995a, 1997; Plank, 1997) and mapping associated with this study. Black triangles indicate geothermal and temperature gradient wells. Temperature gradient contours shown are from (Bergman et al., 2015), thick black line is the 80°C/km contour, dashed line is the 120°C/km contour.**

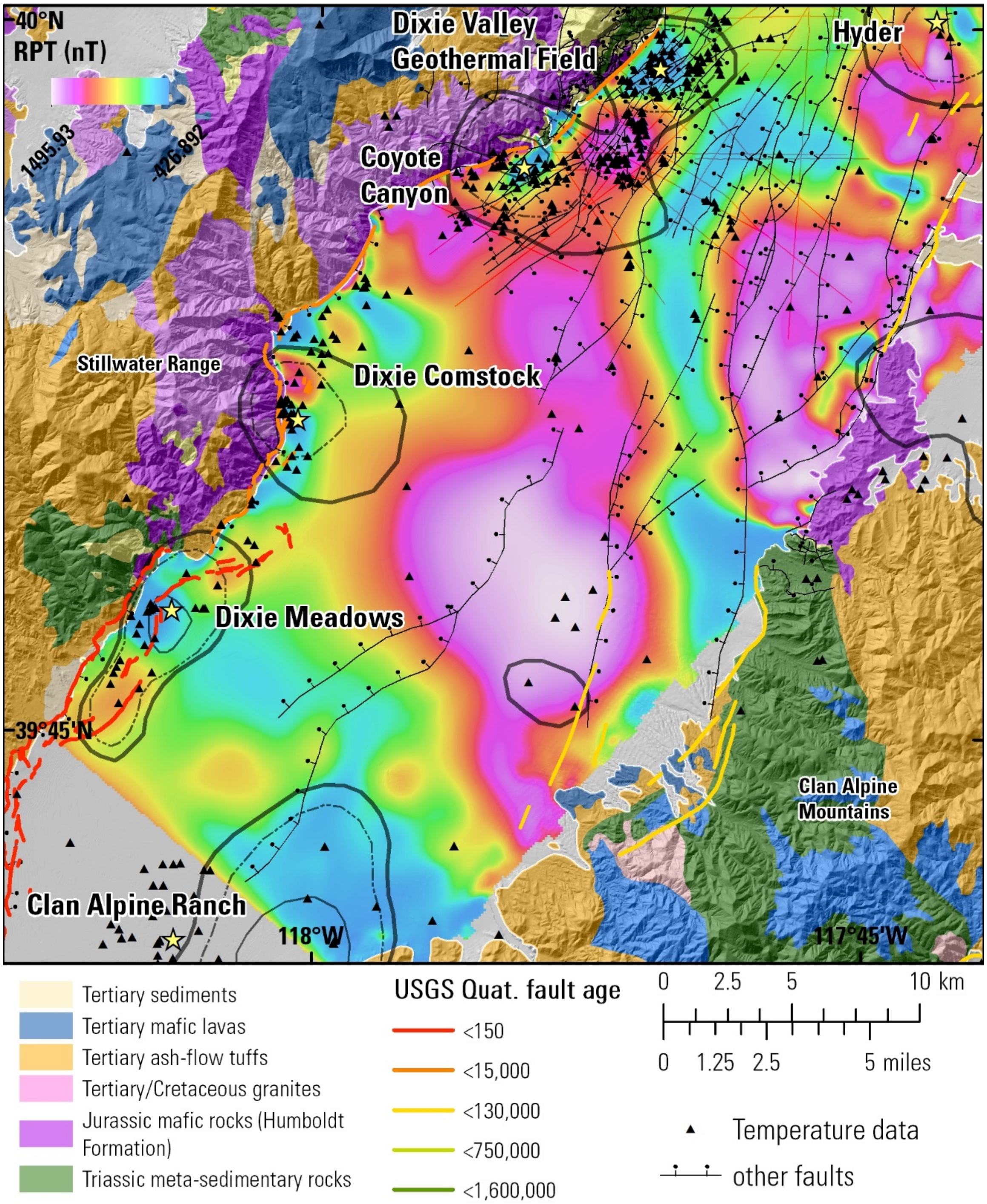


**Figure 5. Magnetic and geologic map of central Dixie Valley. Reduced to pole magnetic anomaly is shown, warm colors indicate magnetic highs, cool colors magnetic lows. Faults (U.S. Geological Survey, 2006) and interpretations of geophysical and geologic data associated with this study are shown. Geology in the ranges from a compilation of maps including (Muller et al., 1951; Page, 1965; Speed, 1976; John, 1995a, 1997; Plank, 1997) and mapping associated with this study. Black triangles indicate geothermal and temperature gradient wells. Temperature gradient contours shown are from (Bergman et al., 2015), thick black line is the 80°C/km contour, dashed line is the 120°C/km contour.**

Scarps associated with the 1954 Dixie Valley earthquake pass immediately west of the Dixie Meadows springs, and along the Stillwater Range front. These scarps terminate a few km north of the Dixie Meadows area. As indicated by gravity data, the eastern set of 1954 scarps is probably associated with the piedmont fault system, which is ~1.0-1.5 km valley-ward of the Dixie Valley range front fault system, similar to the location of the piedmont fault at Dixie Comstock, Coyote Canyon, and the Dixie Valley geothermal field. The Dixie Meadows area lies within a ~1.0-1.5 km-wide right-step in both the Dixie Valley and the piedmont fault systems, as evident from gravity and magnetic data (Figures 4 and 5) as well as the traces of the 1954 ruptures (U.S. Geological Survey, 2006). A magnetic low occurs at Dixie Meadows (Figure 5). Dixie Meadows lies south of the southern termination of exposures of the Humboldt Formation, and is south of the most prominent magnetic body in the valley, which is likely associated with the highly magnetic mafic rocks Humboldt Formation (Grauch, 2002). Based on adjacent outcrops in the Stillwater Range the geology at depth is likely dominated by Triassic meta-sedimentary rocks and Tertiary ash-flow tuffs (Speed, 1976).

### *2.10 Clan Alpine Ranch*

The Clan Alpine Ranch geothermal system is located ~12 km due south of Dixie Meadows hot springs. Clan Alpine Ranch is a blind system defined by ~100 m deep temperature gradient wells. The hottest measured temperature is 72°C at 70 meters depth (Bergman et al., 2015). Bergman et al. (2015) show the Clan Alpine Racnh temperature anomaly along the eastern side of the topographic valley, where as Faulds et al., (2011) indicate that the geothermal system is located near the center of the valley. Nevada Division of Minerals well database show the majority temperature gradient wells in the Clan Alpine Ranch in the center of the valley, though several are located to the east, where the Bergman et al., (2015) temperature gradient anomaly is located. It is therefore unclear if Clan Alpine Ranch is associated with structure on the east or west side of the valley (Figure 6).

To the east of the Clan Alpine Ranch area lies an ~8 km-wide right step in the range front of the Clan Alpine Mountains. This right-step geometry is evident in the Dixie Valley basin as displayed by the gravity data and in the topography of the Clan Alpine Mountains. Mapped faults to the south of the step-over are younger than early Pleistocene (<1.6 Ma), whereas faults to the north of the step are younger than mid-Pleistocene (<130,000 yrs) (U.S. Geological Survey, 2006). No faults are mapped at the topographic range front through the step. This step-over may be too wide to generate a dense, interconnected fault and fracture network that would be conducive to geothermal circulation (e.g., Siler et al., 2018). To the west of Clan Alpine Ranch geothermal area lies the ‘The Bend’ in the Dixie Valley range front fault system. Scarps associated with the 1954 Dixie Valley earthquake along the Dixie Valley fault system follow the range front across a ~90° turn from ~350° to 080° through the ‘The Bend’. Scarps that appear to be associated with the piedmont fault system, strike ~000-010, bridging the The Bend (Figure 6). Tertiary ash-flow tuffs are exposed in the Clan Alpine Mountains to the east, whereas Tertiary granitic rocks, Triassic meta-sedimentary rocks, and Tertiary ash-flow tuffs are exposed in the Stillwater Range to the west. These likely represent the crystalline rock beneath Clan Alpine Ranch.

### *2.11 Pirouette Mountain*

The Pirouette Mountain geothermal area lies ~20 km south-southwest of Clan Alpine Ranch area. The system is blind and is defined by a ~9 km long thermal anomaly outlined by a number of temperature gradient wells (Lazaro et al., 2011). Maximum measure temperatures are 88°C at ~100 m depth. Deep drilling (2250 m) has not encountered elevated temperatures (Lazaro et al., 2011; Bergman et al., 2015).

The Pirouette Mountain area lies amongst a number of fault scarps associated with both the 1954 Dixie Valley and 1954 Fairview Peak earthquakes (Wallace et al., 1984; Caskey et al., 1996; U.S. Geological Survey, 2006). These include scarps along the Gold King, Louderback Mountains, and West Gate faults, all associated with the northern extent of the Fairview Peak event, and scarps along the Dixie Valley fault system associated with the southern extent of Dixie Valley event (Figure 6). Analysis of geologic mapping, LiDAR, hyperspectral imaging, seismic reflection data, magnetotelluric data, and shallow temperature data have been utilized to assess the subsurface structural and temperature characteristics of the Pirouette Mountain area (John, 1995b, 1995a, 1997; Helton et al., 2011; Lamb et al., 2011; Lazaro et al., 2011; Skord et al., 2011; Alm et al., 2016; Unruh et al., 2016). The fault systems defined by these studies describe a complexly faulted area generally characterized by an anticlinal accommodation zone between west-dipping faults to the east and east-dipping faults to the west. (Alm et al., 2016; Unruh et al., 2016). This structure is expressed as a broad gravity high spanning the valley between the Pirouette Mountain and Eleven Mile Canyon geothermal areas. Well 66-16 at Pirouette Mountain penetrated Tertiary silicic volcanic rocks to 1933 m overlying quartzite to 2170 m, overlying granodiorite to total depth at 2250 m (publicly available data Nevada Division of Minerals). The ash-flow tuffs, granodiorite and meta-sedimentary rocks probably represent the reservoir rocks at depth and correlate with units exposed in the Clan Alpine Mountains to the east (John, 1997) and Stillwater Range to the west (John, 1995a).

### *2.12 Eleven Mile Canyon*

The Eleven Mile Canyon geothermal area lies ~12 km south-southeast of Pirouette Mountain and ~15 km north of US highway 50 at the mouth of Eleven Mile Canyon. Eleven Mile Canyon geothermal area is defined by temperature gradient wells and several deeper exploration wells. Maximum measured temperatures are 62°C at ~400 m (Lazaro et al., 2011; Bergman et al., 2015). Deep drilling (~2500 m) has not encountered elevated temperatures (Lazaro et al., 2011; Bergman et al., 2015).

The Eleven Mile Canyon area sits near the southern termination of the surface ruptures associated with the 1954 Dixie Valley earthquake and within a ~10 km-wide zone that links the Dixie Valley earthquake ruptures to the west with ruptures along the Gold King, Louderback Mountains, and West Gate faults to the east, the latter three associated with the northern extent of the Fairview Peak earthquake. The anticlinal accommodation zone between the east-dipping Dixie Valley fault and the west-dipping Gold King, Louderback Mountains, and West Gate faults extends south from the Pirouette Mountain area into the Eleven Mile Canyon area, expressed as a broad gravity high (Figure 6). At the broadest scale, both the Fairview fault and Dixie Valley fault are east-dipping, in a ~13 km wide left-step geometry, though this step-over may be too wide to be a significant control on local permeability generation (e.g., Siler et al., 2018). Within the stepover both east- and west-dipping faults define the anticlinal accommodation zone and several small graben (Mankhemthong et al., 2008; Helton et al., 2011). The dextral-normal slip associated with the Fairview earthquake suggests that the broad left-step has a restraining geometry. Tertiary ash-flow tuffs, and Triassic meta-sedimentary rocks exposed in the Clan Alpine Mountains to the east (John, 1997) and Stillwater Range to the west (John, 1995a) are likely to comprise the crystalline basement beneath Eleven Mile Canyon.

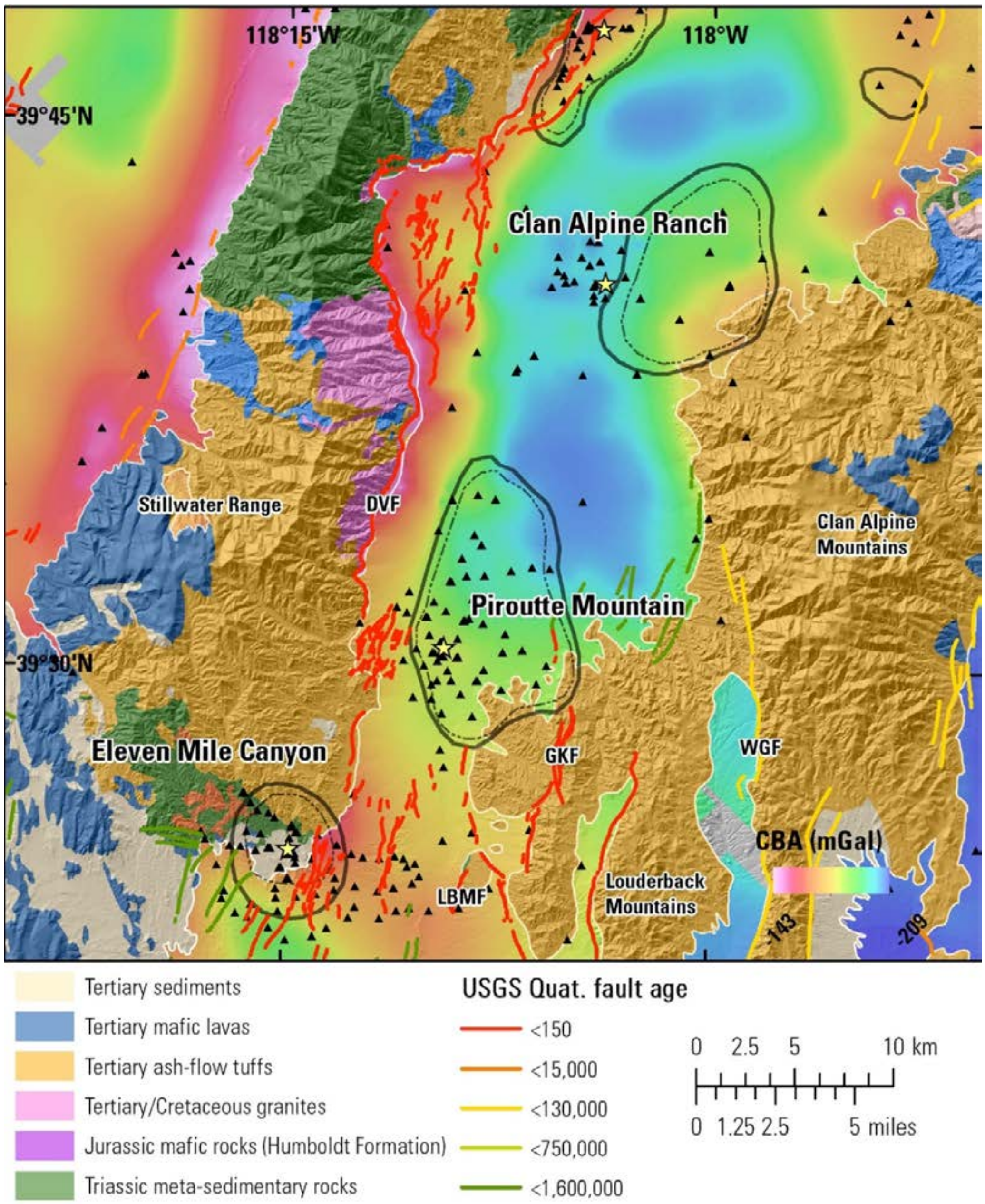


**Figure 6. Gravity and geologic map of southern Dixie Valley. Bouger gravity anomaly is shown, warm colors indicate gravity highs, cool colors gravity lows. Faults (U.S. Geological Survey, 2006) are shown. Geology in the ranges from a compilation of maps including (Muller et al., 1951; Page, 1965; Speed, 1976; John, 1995a, 1997; Plank, 1997) and mapping associated with this study. Black triangles indicate geothermal and temperature gradient wells. Temperature gradient contours shown are from (Bergman et al., 2015), thick black line is the 80°C/km contour, dashed line is the 120°C/km contour.**

## 3. Valley wide themes

All eleven of the geothermal systems in Dixie Valley are associated with structural discontinuities along faults that are younger than mid-Pleistocene. The systems occur at fault step-overs, accommodation zones, and fault intersections. In several cases there are two or more 'nested' discontinuities at different scales generating a more advantageous hybrid structural setting (e.g., Faulds et al., 2013). All eleven geothermal systems are also associated with normal faults striking north-to-northeast (000-045), generally orthogonal to the Quaternary extension direction (west-northwest-to-east-southeast) through central Nevada. Pirouette Mountain and Eleven Mile Canyon may also be associated with dextral-normal displacement as evidenced their proximity to scarps associated with 1954 dextral-normal Fairview peak earthquake.

The three systems with the highest measured temperatures (Dixie Valley geothermal field, Coyote Canyon, and Dixie Comstock occur closely associated with the mafic intrusive/extrusive Humboldt Formation (deep wells at both Dixie Comstock and Coyote Canyon had relatively low flow rates, though the very high measured temperatures may suggest nearby convection). Bergman (2015) suggest that the Humboldt Formation is the dominant faulted reservoir lithology in the Dixie Valley geothermal field. The Humboldt Formation occurs in a ~20 km wide, north-northwest striking zone across the valley, with ~2 km wide magnetic low bisecting it. Overlapping gradients in the magnetic and gravity data suggest this magnetic 'trough' is structurally controlled (Figure 5). Triassic meta-sedimentary rocks are mapped throughout the ranges bounding Dixie Valley and we infer that they may be present at depth beneath all eleven of the known Dixie Valley geothermal systems. If the lack of permeability in the fine-grained and carbonate rich Triassic meta-sedimentary section within the Dixie Valley geothermal field is an indication, the Triassic section may not support sufficient fracture permeability when faulted to conduct large-scale circulation. The coarse-grained, clastic lithologies within the Triassic section mapped throughout the ranges surrounding Dixie Valley may be more prospective.

The piedmont fault system, the fault system which is basin-ward of the Dixie Valley fault along the Stillwater Range front is present from as far south as Pirouette Mountain to as far north as the northern end of the topographic Dixie Valley basin. The piedmont fault ruptured from Pirouette Mountain to north of Dixie Meadows (~35 km) during the 1954 Dixie Valley earthquake. At least six of the eleven geothermal systems and all the systems on the western side of Dixie Valley; Piroutte Mountain, Clan Alpine Ranch, Dixie Meadows, Dixie Comstock, Coyote Canyon, and Dixie Valley geothermal field appear to be associated with the piedmont fault (rather than the Dixie Valley fault at the topographic range front).

All the geothermal systems covered by high-resolution aeromagnetic data, (Dixie Comstock, Dixie Meadows, Coyote Canyon, Dixie Valley geothermal field, and perhaps Hyder), are within or directly adjacent to local magnetic lows (Figures 3 and 5). These lows may be associated with hydrothermal alteration of magnetic minerals (Grauch, 2002; Bergman et al., 2015; Earney et al., this volume).

The apparent significance of the piedmont fault to geothermal occurrence, and its lack of surface exposure in the northern part of the valley, as well as the local magnetic lows that are associated with all systems over which detailed magnetic data are available, attest to the utility of potential-field geophysical data in characterizing the structure of geothermal systems. In concert with surficial structural mapping, gravity and magnetic data are crucial for developing a complete understanding structural controls of geothermal systems. These techniques help to characterize both basin-scale and local-scale structure and, in the case of the local magnetic lows, may identify locations in the subsurface that are generated by geothermal circulation.

## 4. Conclusions

Dixie Valley in central Nevada hosts and seemingly anomalously high number of geothermal systems with respect to the Basin and Range. Each geothermal thermal system appears to be geochemically and hydrogeologically distinct, though perhaps all are generally related to a very deep source (Bergman et al., 2015). The regionally high heat flow, strain-rates, $^3He/^4He$ in geothermal fluids, and historic seismicity suggests that regional tectonics certainly exerts some control on the abundance of geothermal systems in Dixie Valley. The density of geothermal systems in Dixie Valley, relative to neighboring valleys (Figure 1) suggests that there are also local characteristics that control the individual circulation cells associated with these systems. The abundance of *recognized* geothermal systems in Dixie Valley may be related to basin hydrogeology. The relative relief between Dixie Valley and the bounding ranges, results in relative high hydrologic head in some parts of the valley and a number of artesian wells and springs. The interaction between deeply derived thermal fluids and ground water at very shallow levels may be the primary reason behind the discovery of several of the Dixie Valley geothermal systems (as surface springs and shallow temperature anomalies) (Bergman et al., 2015).

The complex structural discontinuities along relatively young fault systems are clearly intimately associated with geothermal systems in Dixie Valley. The adjacency of the highest temperature systems with Jurassic igneous rocks suggests that host lithology plays an important role in localizing fluid circulation as well. Still, the Humboldt Formation is mapped across several ranges in central Nevada (Speed, 1976) it is certainly not the only formation to host geothermal systems. Though the faults in Dixie Valley are young relative to surrounding basins, the geothermal systems are thought to relatively long-lived (~100 ka; Bergman et al., 2015), and complex fault structure is certainly not unique to Dixie Valley. This information together implies that the structural and geologic character of Dixie Valley are not out of the ordinary, and that other neighboring basins, affected by analogous regional heat and strain patterns, may support a similar density of geothermal systems, which are as yet unrecognized because fluids do not circulate to shallow enough levels for detection.

## REFERENCES

Alm, S., Walker, J.D., Blake, K., 2016. Structural complexity of the Pirouette Mountain and Elevenmile Canyon Geothermal Systems. Geothermal Resources Council Transactions 40, 433–438.

Bell, J.W., Caskey, S.J., Ramelli, A.R., Guerrieri, L., 2004. Pattern and Rates of Faulting in the Central Nevada Seismic Belt , and Paleoseismic Evidence for Prior Beltlike Behavior. Bulletin of the Seismological Society of America 94, 1229–1254.

Benoit, W.R., 2011. The Geothermal Systems in Dixie Valley, Renewable Energy Churchill County. http://www.churchillcounty.org/DocumentCenter/View/5354.

Bergman, S.C., Blackwell, D.D., Goff, F., Kennedy, B.M., McKenna, J.R., Richards, M.C., Smith, R.P., Waibel, A.F., Wannamaker, P.E., 2015. Dixie Valley Synthesis. SMU Geothermal Laboratory, Dallas, TX.

Blackwell, D.D., Golan, B., Benoit, D., 2000. Thermal regime in the Dixie Valley geothermal system. Geothermal Resources Council Transactions 24, 223–228.

Blackwell, D.D., Smith, R.P., Richards, M.C., 2007. Exploration and Development at Dixie Valley, Nevada: Summary of DOE Studies. Proceedings, Thirty-Second Workshop on Geothermal Reservoir Engineering Stanford University. 16.

Blakely, R.J., 1996. Potential theory in gravity and magnetic applications. Cambridge University Press.

Bohm, B.W., Jacobson, R.L., Campana, M.E., Ingraham, N.L., 1980. Hydrology and Hydrogeochemistry: Geothermal Reservoir Assessment Case Study, Northern Basin and Range Province, Northern Dixie Valley, Nevada. Mackay Minerals Research Institute.

Caskey, S.J., Bell, J.W., Ramelli, A.R., Wesnousky, S.G., 2004. Historic Surface Faulting and Paleoseismicity in the Area of the 1954 Rainbow Mountain – Stillwater Earthquake Sequence, Central Nevada. Bulletin of the Seismological Society of America 94, 1255–1275.

Caskey, S.J., Ramelli, A.R., 2004. Tectonic displacement and far-field isostatic flexure of pluvial lake shorelines, Dixie Valley, Nevada. Journal of Geodynamics 38, 131–145.

Caskey, S.J., Wesnousky, S.G., Zhang, P., Slemmons, D.B., 1996. Surface faulting of the 1954 Fairview Peak (MS 7.2) and Dixie Valley (MS 6.8) earthquakes, central Nevada. Bulletin of the Seismological Society of America 86, 761–787.

Faulds, J.E., Coolbaugh, M., Blewitt, G., Henry, C.D., 2004. Why is Nevada in hot water? Structural controls and tectonic model of geothermal systems in the northwestern Great Basin. Geothermal Resources Council Transactions 28, 649–654.

Faulds, J.E., Coolbaugh, M.F., Vice, G.S., Edwards, M.L., 2006. Characterizing Structural Controls of Geothermal Fields in the Northwestern Great Basin: A Progress Report. Geothermal Resources Council Transactions 30, 69–76.

Faulds, J.E., Hinz, N.H., 2015. Favorable Tectonic and Structural Settings of Geothermal Systems in the Great Basin Region, western USA: Proxies for Discovering Blind Geothermal Systems. Proceedings of the World Geothermal Congress. 6.

Faulds, J.E., Hinz, N.H., Coolbaugh, M.F., Cashman, P.H., Kratt, C., Dering, G.M., Edwards, J., Mayhew, B., Mclachlan, H., 2011. Assessment of Favorable Structural Settings of Geothermal Systems in the Great Basin, Western USA. Geothermal Resources Council Transactions 35, 777–784.

Faulds, J.E., Hinz, N.H., Coolbaugh, M.F., Shevenell, L.A., Siler, D.L., 2016. The Nevada play fairway project-phase II: Initial search for new viable geothermal systems in the great basin region, western USA. Geothermal Resources Council Transactions.

Faulds, J.E., Hinz, N.H., Dering, G.M., Siler, D.L., 2013. The Hybrid Model — The Most Accommodating Structural Setting for Geothermal Power Generation in the Great Basin, Western USA. Geothermal Resources Council Transactions 37, 4–10.

Faulds, J.E., Hinz, N.H., Sadowski, A., Ramelli, A.R., Mlwasky, E., McConville, E., Craig, J., Bourdeau-Hernikl, J., Shevenell, L.A., Coolbaugh, M.F., Hardwick, C.L., Gwynn, M., Allis, R., Siler, D.L., Queen, J.H., Lide, C., Spycher, N.F., 2017. Discovering Blind Geothermal Systems in the Great Basin Region: An integrated Geologic and Geophysical Approahc for Establishing Geothermal Play Fairways: Budget Period 2.

Goff, F., Bergfeld, D., Janik, C.J., Counce, D., Murrell, M., 2002. Geochemical Data on Waters, Gases, Scales, and Rocks from the Dixie Valley Region, Nevada (1996-1999). Los Alamos National Lab, LA-1 3972-MS.

Grauch, V.J.S., 2002. High-resolution aeromagnetic survey to image shallow faults, Dixie Valley geothermal field, Nevada. US Department of the Interior, US Geological Survey Open-File Report 02-384.

Hammond, W.C., Blewitt, G., Kreemer, C., 2014. Steady contemporary deformation of the central Basin and Range Province, western United States. Journal of Geophysical Research, Solid Earth 119. https://doi.org/10.1002/2014JB011145

Helton, E.L., Bell, J.W., Cashman, P.H., Lazaro, M., Alm, S., 2011. Structural analysis of southern Dixie Valley using LiDAR and low-sun-angle aerial photography, NAS Fallon Geothermal Exploration Project, Dixie Valley, Nevada. Geothermal Resources Council Transactions 35, 811–815.

Iovenitti, J., Sainsbury, J., Tibuleac, I., Karlin, R., Wannamaker, P.E., Maris, V., Thakur, M., Ibser, F.H., Lewicki, J., Kennedy, B.M., Swyer, M., 2013. EGS exploration methodology project using the Dixie Valley geothermal system, Nevada, status update. Proceedings, Thirty-Eighth Workshop on Geothermal Reservoir Engineering, Stanford University 38, 826–835.

John, D.A., 1997. Geology of the Wonder Mountain quadrangle. Churchill County, Nevada: Nevada Bureau of Mines and Geology Map 109.

John, D.A., 1995a. Geologic map of the Pirouette Mountain quadrangle. Nevada Bureau of Mines and Geology Field Studies Map 9.

John, D.A., 1995b. Tilted middle Tertiary ash-flow calderas and subjacent granitic plutons, southern Stillwater Range, Nevada: Cross sections of an Oligocene igneous center. Geological Society of America Bulletin 107, 180–200.

Johnson, S.D., Hulen, J.B., 2002. Subsurface stratigraphy, structure, and alteration in the Senator thermal area, northern Dixie Valley geothermal field, Nevada. Geothermal Resources Council Transactions 26, 533–542.

Kennedy-Bowdoin, T., Silver, E., Martini, B., Pickles, W., 2004. Geothermal prospecting using hyperspectral imaging and field observations, Dixie Meadows, NV. Geothermal Resources Council Transactions 28, 10.

Kennedy, B.M., van Soest, M.C., 2007. Flow of Mantle Fluids Through the Ductile Lower Crust: Helium Isotope Trends. Science 318, 1433–1436. https://doi.org/10.1126/science.1147537

Kennedy, B.M., van Soest, M.C., 2006. A helium isotope perspective on the Dixie Valley, Nevada, hydrothermal system. Geothermics 35, 26–43. https://doi.org/10.1016/j.geothermics.2005.09.004

Kreemer, C., Blewitt, G., Hammond, W.C., 2009. Geodetic constraints on contemporary deformation in the northern Walker Lane : 2 . Velocity and strain rate tensor analysis W a t. In: Oldow, J.S., Cashman, P.H. (Eds.), Late Cenozoic Structure and Evolution of the Great Basin Sierra Nevada Transition. Geologic Society of America Special Paper 447, 17–31. https://doi.org/10.1130/2009.2447(02).

Kreemer, C., Hammond, W.C., Blewitt, G., Holland, A.A., Bennett, R.A., 2012. A Geodetic Strain Rate Model for the Pacific – North American Plate Boundary, Western United States: Nevada Bureau of Mines and Geology, Reno, Nevada.

Lamb, A., Kratt, C., Calvin, W., 2011. Geothermal exploration using hyperspectral analysis over Dixie and Fairview Valleys, Nevada. Geothermal Resources Council Transactions 35, 867–871.

Lazaro, M., Alm, S., Tiedeman, A., Page, C., Meade, D., Shoffner, J., Bucher, K., 2011. Department of the Navy Geothermal Exploration on Naval Air Station Fall (NASF) Managed Lands in Dixie Valley, Nevada. Geothermal Resources Council Transactions 35.

Mankhemthong, N., Oppliger, G.L., Aslett, Z., 2008. Structural Localization of Two Low Temperature Geothermal Systems Within the Gravity Defined Linkage Between Dixie Valley and Fairview Valley, Nevada, USA. Geothermal Resources Council Transactions 32, 291–295.

Muller, S.W., Ferguson, H.G., Roberts, R.J., 1951. Geology of the Mount Tobin quadrangle, Nevada. US Geological Survey.

Page, B.M., 1965. Preliminary geologic map of a part of the Stillwater Range, Churchill County, Nevada. Nevada Bureau of Mines & Geology Map 28.

Plank, G.L., 1997. Geologic map of the Stillwater Escarpement above the Dixie Valley Geothermal Site; unpublished map.

Ponce, D.A., 1997. Gravity data of Nevada. US Department of the Interior, US Geological Survey.

Rowan, L.C., Wetlaufer, P.H., 1981. Relation Between Regional Lineament Systems and Structural Zones in Nevada. AAPG Bulletin 65, 1414–1432.

Siler, D.L., Hinz, N.H., Faulds, J.E., 2018. Stress concentrations at structural discontinuities in active fault zones in the western United States: Implications for permeability and fluid flow in geothermal field. Geological Society of America Bulletin. https://doi.org/https://doi.org/10.1130/B31729.1

Siler, D.L., Kennedy, B.M., 2016. Regional crustal-scale structures as conduits for deep geothermal upflow. Geothermics 59, 27–37. https://doi.org/10.1016/j.geothermics.2015.10.007

Skord, J., Sladek, C., Coolbaugh, M., Cashman, P.H., Lazaro, M., Kratt, C., 2011. Two Meter Temperature Surveys for Geothermal Exploration Project at NAS Fallon. Geothermal Resources Council Transactions 35, 1023–1027.

Slemmons, D.B., 1957. Geological effects of the Dixie Valley-Fairview Peak Nevada, Earthquakes of December 16, 1954. Bulletin of the Seismological Society of America 47, 353–357.

Speed, R.C., 1976. Geologic map of the Humboldt lopolith and surrounding terrian, Nevada. Geoloigc Society of America Map MC-14; scale ~1:80,000.

U.S. Geological Survey, 2006. Quaternary Fault and Fold Database for the United States, accessed February 2014, from U.S. Geological Survey website: http//earthquakes.usgs.gov/regional/qfaults/.

Unruh, J., Gray, B., Christopherson, K., Pullammanappallil, S., Alm, S., Blake, K., 2016. Seismic Reflection and Magnetotelluric Imaging of Southwestern Dixie Valley Basin, Nevada. Geothermal Resources Council Transactions 40, 455–461.

Vikre, P.G., 1994. Gold mineralization and fault evolution at the Dixie Comstock Mine, Churchill County, Nevada. Economic Geology 89, 707–719.

Wallace, R.E., Bonilla, M., A, V.H., 1984. Fault scarps formed during the earthquakes of October 2, 1915, in Pleasant Valley, Nevada, and some tectonic implications. U.S. Geological Survey Professional Paper 1274-A,B.

Williams, C.F., DeAngelo, J., 2011. Evaluation of Approaches and Associated Uncertainties in the Estimation of Temperatures in the Upper Crust of the Western United States. Geothermal Resources Council Transactions 25.

Williams, C.F., Sass, J.H., Grubb, F. V, 1997. Thermal signature of subsurface fluid flow in the Dixie Valley geothermal field, Nevada. Proceedings, Twenty-Second Workshop on Geothermal Reservoir Engineering, Stanford University. 161–168.

Wisian, K.W., Blackwell, D.D., 2004. Numerical modeling of Basin and Range geothermal systems. Geothermics 33, 713–741. https://doi.org/10.1016/j.geothermics.2004.01.002